

Solution Structure of the Monovalent Lectin Microvirin in Complex with Man α (1–2)Man Provides a Basis for Anti-HIV Activity with Low Toxicity^{*[5]}

Received for publication, February 17, 2011, and in revised form, March 23, 2011 Published, JBC Papers in Press, April 6, 2011, DOI 10.1074/jbc.M111.232678

Syed Shahzad-ul-Hussan[‡], Elena Gustchina[§], Rodolfo Ghirlando[¶], G. Marius Clore[§], and Carole A. Bewley^{‡1}

From the [‡]Laboratory of Bioorganic Chemistry, [§]Laboratory of Chemical Physics, and the [¶]Laboratory of Molecular Biology, NIDDK, National Institutes of Health, Bethesda, Maryland 20892

Lectins that bind surface envelope glycoprotein gp120 of HIV with high avidity can potently inhibit viral entry. Yet properties such as multivalency that facilitate strong interactions can also cause nonspecific binding and toxicity. The cyanobacterial lectin microvirin (MVN) is unusual as it potently inhibits HIV-1 with negligible toxicity compared with cyanovirin-N (CVN), its well studied antiviral homolog. To understand the structural and mechanistic basis for these differences, we solved the solution structure of MVN free and in complex with its ligand Man α (1–2)Man, and we compared specificity and time windows of inhibition with CVN and Man α (1–2)Man-specific mAb 2G12. We show by NMR and analytical ultracentrifugation that MVN is monomeric in solution, and we demonstrate by NMR that Man α (1–2)Man-terminating carbohydrates interact with a single carbohydrate-binding site. Synchronized infectivity assays show that 2G12, MVN, and CVN inhibit entry with distinct kinetics. Despite shared specificity for Man α (1–2)Man termini, combinations of the inhibitors are synergistic suggesting they recognize discrete glycans and/or dynamic glycan conformations on gp120. Entry assays employing amphotropic viruses show that MVN is inactive, whereas CVN potently inhibits both. In addition to demonstrating that HIV-1 can be inhibited through monovalent interactions, given the similarity of the carbohydrate-binding site common to MVN and CVN, these data suggest that gp120 behaves as a clustered glycan epitope and that multivalent-protein interactions achievable with CVN but not MVN are required for inhibition of some viruses.

Human immunodeficiency virus (HIV) infections continue to exert an enormous toll on global human health. Advances in drug therapies can extend life expectancies of HIV-infected patients to be comparable with noninfected individuals, but their outcome can nevertheless be compromised by disparate access to antiretrovirals and resistance to

approved anti-HIV drugs (1). These circumstances have led experts to emphasize the importance of developing new measures for preventing HIV infections (2). In addition to vaccine development, an approach that shows exceptional promise involves targeting the “glycan shield” of surface envelope proteins for HIV to inhibit membrane fusion and infection (3).

The initial steps leading to viral entry include binding of the HIV surface envelope glycoprotein gp120 to cellular receptors CD4 and CXCR4 or CCR5, followed by gp41-mediated membrane fusion (4). Although gp120 is largely responsible for target cell engagement through several highly conserved epitopes, a large portion of its surface is masked by complex-type and high mannose-type carbohydrate structures. Across clades, gp120 contains on average more than 20 *N*- and *O*-linked glycosylation sites that account for ~50% of its molecular mass (5–7). This dense display of host-processed glycans functions as a barrier to protect the virus from recognition by the human immune system (8). To exploit this barrier as a therapeutic target, carbohydrate-binding proteins, known as lectins, have emerged as promising anti-HIV agents (3, 9, 10). A number of lectins and at least one monoclonal antibody, 2G12, potently block HIV infection at the initial stage of membrane fusion by binding carbohydrate structures present on gp120 (11–14), providing support for this approach.

The avidity of carbohydrate-mediated interactions increases through multivalent binding (15, 16). Engendered in their tertiary or quaternary structures, lectins often contain two or more carbohydrate recognition sites that might allow for simultaneous binding to multiple arms of a branched carbohydrate and/or to separate proximal carbohydrates present on cell surfaces (11, 17, 18). Alternatively, recent studies revealing the basis for high avidity single site interactions through a “bind-and-hop” mechanism occurring with clustered glycan epitopes explain a separate mechanism for carbohydrate-mediated interactions (19, 20).

Within the past decade, a number of new plant and bacterial lectins have been described that are capable of inhibiting HIV entry with potencies at low to subnanomolar ranges. Several are under preclinical development as topical microbicides to prevent sexual transmission of HIV and to show efficacy in primate challenge models (9, 10). Challenges to developing lectins for clinical use include large scale production and demonstration of a lack of toxicity and immunogenicity. The cyanobacterial

* This work was supported, in whole or in part, by National Institutes of Health Intramural Research Program (NIDDK) and the Intramural AIDS Targeted Antiviral Program of the Office of the Director (to C. A. B. and G. M. C.).

[5] The on-line version of this article (available at <http://www.jbc.org>) contains supplemental Figs. S1–S10, Tables S1–S3, and additional references.

The atomic coordinates and structure factors (code 2y1s) have been deposited in the Protein Data Bank, Research Collaboratory for Structural Bioinformatics, Rutgers University, New Brunswick, NJ (<http://www.rcsb.org/>).

¹ To whom correspondence should be addressed: 8 Center Dr., Bethesda, MD 20892-0820. Fax: 301-401-4182; E-mail: caroleb@mail.nih.gov.

protein microvirin (MVN)² (21) is an attractive candidate for microbicide development; when compared with its well studied homolog cyanovirin-N (CVN), it is reported to show comparable potency in HIV-1 neutralization assays but with notably reduced toxicity profiles (22). To determine the molecular basis for antiviral activity, carbohydrate specificity, and low toxicity, we have characterized the biophysical properties of MVN and solved the solution structure of MVN free and in complex with Man α (1–2)Man. These studies demonstrate that recombinant MVN is monovalent with respect to oligomannose binding, which precludes intermolecular oligomerization or cross-linking in the presence of these branched carbohydrates. Neutralization studies with MVN, CVN, and 2G12, all of which bind Man α (1–2)Man, reveal new insights into carbohydrate-mediated inhibition of HIV-1 entry.

EXPERIMENTAL PROCEDURES

Production and Biophysical Characterization of Recombinant Proteins—A synthetic gene encoding MVN (GeneArt) was cloned into pET-15b and ¹⁵N- or ¹⁵N/¹³C-uniformly labeled recombinant protein expressed in M9 media using standard methods. CVN was expressed and purified as described previously (23). All protein samples used in NMR and microcalorimetry experiments or infectivity assays were subjected to a final purification step by size exclusion chromatography eluting with 20 mM NaPO₄, 50 mM NaCl, pH 6.85 (NMR buffer), and the oligomeric state of each sample was confirmed by analytical ultracentrifugation and NMR relaxation experiments prior to use. Protein concentrations were quantified by absorbance at 280 nm using a molar extinction coefficient of 18,000 M⁻¹ cm⁻¹. Monoclonal antibodies 2G12 and C34 were purchased from Polymun and American Peptide, respectively. Isothermal titration calorimetry (ITC) experiments were performed as described previously (24).

Analytical Ultracentrifugation of MVN—Sedimentation velocity experiments were conducted at 20.0 °C on a Beckman Optima XL-A analytical ultracentrifuge. Samples of ¹⁵N-labeled MVN dissolved in NMR buffer, purified by size exclusion chromatography, were loaded at 15, 30, and 60 μ M into two-channel, 12-mm path length sector-shaped cells (400 μ L). 220 scans were acquired at 3.5-min intervals and rotor speeds of 50,000 rpm with data collected as single absorbance measurements at 280 nm using a radial spacing of 0.003 cm. Data were analyzed in SEDFIT 12.1 (25) in terms of a continuous *c*(*s*) distribution. The solution density, ρ , and viscosity, η , were calculated using SEDNTERP 1.09 (26). The protein partial specific volume was determined using SEDNTERP 1.09 and corrected for the ¹⁵N isotopic substitution. The *c*(*s*) analyses were carried out using an *s* range of 0.0 to 5.0 with a linear resolution of 100 and a confidence level (*F* ratio) of 0.68. In all cases, excellent fits were observed with root mean square deviations ranging from 0.0028 to 0.0066 absorbance units. Equally good fits were obtained when data were analyzed in terms of a single nonin-

teracting species, returning identical values for the sedimentation coefficient (1.77 \pm 0.01 S) and molecular mass (12.8 \pm 0.1 kDa). Sedimentation coefficients were corrected to standard conditions at 20.0 °C in water, *s*_{20,w}.

NMR Spectroscopy and Structure Calculations—NMR data were recorded at 300 K on 500 or 600 MHz spectrometers equipped with *z* gradient triple resonance cryoprobes. Data were processed using NMRPipe (27). Spectra used for chemical shift and NOE assignments were analyzed with the programs Sparky and PIPP (28), respectively, and structures were calculated with Xplor-NIH (29) Backbone ϕ and ψ torsion angles were derived from ³J_{HN α values and the program Talos+ (30). ¹D_{NH} residual dipolar couplings (RDCs) for free and bound MVN were obtained by taking the difference in ¹J_{NH} couplings in a dilute liquid crystalline medium (5% PEG (C12E5)/*n*-hexanol (31)) and isotropic medium (NMR buffer) as measured using the in-phase/anti-phase scheme (32). τ_c was determined from the average T₁/T₂ ratio as described previously (33, 34).}

The structure of a 1:1 complex of MVN:Man α (1–2)Man was determined by conjoined rigid body/torsion angle-simulated annealing (35) using Xplor-NIH (29). In this method, the protein backbone along with side chains of residues not involved in carbohydrate binding are held rigid, whereas the side chains of residues involved in carbohydrate binding are given torsional degrees of freedom, and the carbohydrate is given torsional, translational, and rotational degrees of freedom during the calculations (11, 36).

Virus Neutralization and Synchronized Time-of-Addition Neutralization Assays—Env-pseudotyped HIV neutralization assays were performed as described previously (37) using viral particles pseudotyped with HIV-1 envelopes (38). Serial dilutions of inhibitors were added to the pseudovirus, followed by TZM-bl (CXCR4- and CCR5-expressing cells) target cells at 37 °C. 48 h post-infection, cells were lysed, and luciferase activity was measured. A full list of reagents and cell lines appears in the [supplemental material](#).

Synchronized viral infection assays were performed by spinoculation (39, 40) with HIV-1 strain HXB2. Luminescence intensity corresponding to % infection at different time points was converted to percentage of infection relative to positive controls (*Y*_{max}). Data were fit to the sigmoidal equation $Y = Y_{\max}/(1 + \exp(-(t - t_{1/2})/k))$, where *t*_{1/2} is the half-life for the inhibitor-sensitive states of HIV envelope, and *k* is the exponential rate constant.

Synergy Experiments—Neutralizing activities of multiple constant ratio combinations of MVN and CVN or 2G12 were tested in serial dilutions in HXB2 Env-pseudotyped HIV neutralization assays. Combination effects were analyzed as described (41, 42). The dose reduction index (DRI) of inhibitor *x* in combination with inhibitor *y* is given by $DRI_x = (IC_{50})_x / (IC_{50})_{x,y}$, where (IC₅₀)_{*x*} and (IC₅₀)_{*x,y*} are the IC₅₀ values of *x* alone and in combination with *y*, respectively. The combination index (CI) describing the summation of effects of two inhibitors is given by $CI = (DRI_x)^{-1} + (DRI_y)^{-1} + (DRI_x DRI_y)^{-1}$, where the last term, which makes a small contribution to CI, accounts for the state where both inhibitors are bound.

² The abbreviations used are: MVN, microvirin; CVN, cyanovirin-N; DRI, dose reduction index; CI, combination index; ITC, isothermal titration calorimetry; RDC, residual dipolar coupling; DRI, dose reduction index; MLV, murine leukemia virus; VSV, vesicular stomatitis virus.

TABLE 1

Structural statistics for MVN

(SA) are the final 40 simulated annealing structures. SA_r is the restrained regularized mean structure derived from the mean coordinates obtained by averaging the coordinates of the 40 simulated annealing structures best fitted to each other. The number of terms for the various restraints is given in parentheses. r.m.s. indicates root mean square.

	(SA)	SA _r
r.m.s. deviations from experimental restraints		
Distances ^a (986)	0.018 ± 0.002 Å	0.015 Å
Torsion angles ^a (326)	0.65 ± 0.00°	0.25°
³ J _{HNα} coupling constants ^a (40)	0.97 ± 0.02 Hz	0.93 Hz
¹ D _{NH} residual dipolar coupling R factor ^b (55)	1.53 ± 0.07%	1.1%
r.m.s. deviations from idealized covalent geometry		
Bonds	0.005 ± 0.000 Å	0.002 Å
Angles	0.645 ± 0.002°	0.358°
Impropers	0.654 ± 0.034°	0.366°
Measures of structure quality		
E _{LJ} (kcal mol ⁻¹) ^c	-687.6 ± 17.0	-687
PROCHECK ^d		
Residues in most favorable region of Ramachandran plot		89%
No of bad contacts per 100 residues		5
Coordinate precision (Å)^e		
Backbone (N, Cα, C', O)	0.22 ± 0.05	
All non-hydrogen atoms	0.49 ± 0.07	

^a None of the structures exhibited interproton distance violations greater than 0.2 Å, dihedral angle violations greater than 5°, or ³J_{HNα} coupling constant violations greater than 2 Hz. Interproton distance restraints included 148 intraresidue, 321 sequential ($|i - j| = 1$), 138 medium range ($1 < |i - j| < 5$), and 379 long range ($|i - j| > 5$) restraints. Thirty six of these (8 medium range and 28 long range) represent backbone hydrogen bonding restraints for 18 residues (two per hydrogen bond, r_{NH-O} = 1.5–2.8 Å, r_{N-O} = 2.4–3.5 Å) and were introduced during the final stages of refinement on the basis of backbone three-bond couplings.

^b The RDC R-factor (47), which scales between 0 and 100%, is defined as the ratio of the root mean square deviation between observed and calculated values to the expected root mean square deviation if the vectors were randomly distributed, given by $[2Da^2(4 + 3\eta^2)/5]^{1/2}$, where Da is the magnitude of the principal component of the alignment tensor, and η is the rhombicity (59). The values of Da^{NH} and η , derived from the distribution of normalized RDCs, are -17.9 Hz and 0.45, respectively, for the data recorded in PEG/hexanol (31).

^c The Lennard-Jones van der Waals energy was calculated with the CHARMM PARAM19/20 parameters and is not included in the target function for simulated annealing or restrained minimization.

^d The overall quality of the structure was assessed using the program PROCHECK (60). There were no ϕ/ψ angles in the disallowed region of the Ramachandran plot.

^e This is defined as the average root mean square difference (residues 4–104) between the final 40 simulated annealing structures and the mean coordinates.

by two disulfide bonds between Cys-63 and Cys-78 and Cys-60 and Cys-80, and domain B consists of residues 1–37 and 94–108, with one disulfide bond between Cys-8 and Cys-24 (Fig. 2B). At the structural level, MVN differs from CVN in several respects. A two-amino acid insertion in strand β 1 of MVN is propagated through strands β 1 and β 2, making each of the strands in the first β -sheet one residue longer than their equivalents in CVN. In domain A, a four-amino acid insert within the second β -sheet introduces a long, flexible loop between strands β 6 and β 7. Interestingly, the additional disulfide bond relative to CVN occurs between Cys-63/Cys-78 to covalently stabilize strands β 6 and β 7 (44).

Carbohydrate Specificity of MVN—We used a combination of glycan array profiling and NMR spectroscopy to investigate the specificity of MVN for carbohydrates. MVN was initially shown to bind to high mannose-type oligosaccharides using a printed glass slide on which synthetic mannose structures were arrayed (21). Here, fluorescently labeled MVN was screened for carbohydrate binding to a glycan microarray containing nearly 400 diverse carbohydrates, including natural high mannose-type oligosaccharides (46). The profile is shown in supplemental Fig. S2. Although this microarray contains numerous oligomannosides, MVN showed an extremely narrow profile binding to only five glycans on the array. These are characterized by the presence of accessible Man α (1–2)Man α units, structures that terminate the arms of *N*-linked high mannose oligosaccharides such as Man₉GlcNAc₂ and some isomers of Man₈GlcNAc₂.

Specificity was further investigated by NMR titration experiments. Because ¹H and ¹⁵N chemical shifts of backbone amide resonances are sensitive to changes in a chemical environment,

ligand binding can be detected in ¹H-¹⁵N-correlation (HSQC) spectra, and chemical shift perturbations can be mapped directly onto the protein structure to identify the ligand binding site(s). ¹H-¹⁵N HSQC spectra of ¹⁵N-MVN in the presence of increasing amounts of 14 different carbohydrate fragments (supplemental Table S1) present in Man₉GlcNAc₂ were recorded and changes in backbone amide resonances measured. Chemical shift perturbations were observed only with carbohydrates containing a terminal Man α (1–2)Man disaccharide unit (Fig. 3A). ¹H-¹⁵N HSQC spectra of MVN titrated with Man α (1–2)Man-terminating trisaccharides, including Man α (1–2)Man α (1–2)Man, Man α (1–2)Man α (1–3)Man, and Man α (1–2)Man α (1–6)Man (4–6 in supplemental Table S1), were indistinguishable from those with the disaccharide Man α (1–2)Man, indicating specificity for the disaccharide unit.

Mode of Carbohydrate Recognition by MVN—NMR titrations showed MVN binds Man α (1–2)Man in slow exchange on the NMR time scale and that the protein is saturated upon addition of 1 eq of carbohydrate, as the spectra remain unchanged upon addition of stoichiometric excess of ligand. Residues displaying chemical shift perturbations upon binding Man α (1–2)Man were mapped onto the three-dimensional structure of MVN. Surprisingly, these residues were located within a single domain (domain A) of the protein (Fig. 3, B and C). To determine whether other weaker binding sites were present, ¹H-¹⁵N HSQC spectra were recorded on 100 μ M samples titrated with up to a 25-fold stoichiometric excess (2.5 mM) of Man α (1–2)Man or Man α (1–2)Man α (1–2)Man (supplemental Fig. S3). These spectra appeared identical to those

TABLE 2
Binding constants and stoichiometry measured by isothermal titration calorimetry

Glycans	Stoichiometry	K_d M^{-1}	ΔH $kcal\ mol^{-1}$	ΔS $cal\ mol^{-1}$
Man α 1–2Man	0.99	$2.1 (\pm 0.2) \times 10^4$	-7.3 ± 0.3	-4.7
Man α 1–2Man α 1–2Man α Me	0.92	$4.1 (\pm 0.3) \times 10^4$	-8.2 ± 0.2	-6.5
Man α 1–2Man α 1–6Man α Me	0.92	$2.4 (\pm 0.2) \times 10^4$	-7.5 ± 0.3	-5.2
Man $_9$ GlcNAc $_2$	0.91	$1.6 (\pm 0.3) \times 10^5$	-6.3 ± 0.4	2.9

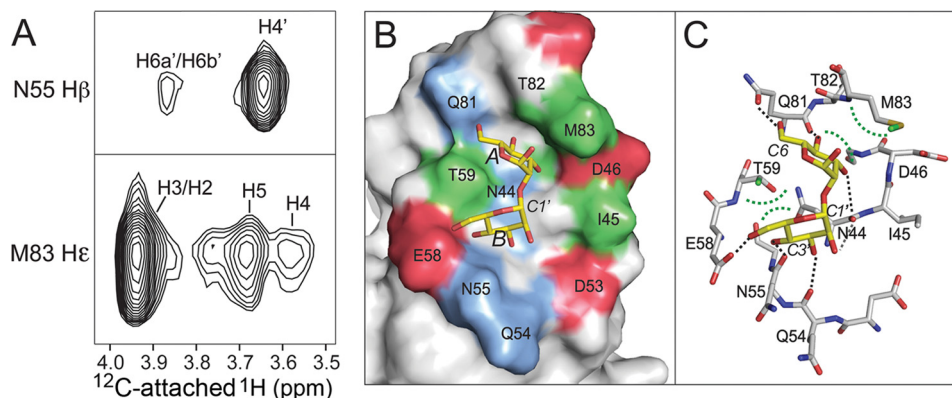


FIGURE 4. Solution structure of MVN in complex with Man α (1–2)Man. *A*, sample planes from a three-dimensional ^{12}C -filtered/ ^{13}C -separated NOE spectrum showing strong intermolecular NOEs between ^{13}C -attached Asn-55 H β and Met-83 H ϵ protons in MVN and ^{13}C -attached protons of α -mannobiose. *B*, close up of the carbohydrate-binding site with MVN shown as a surface representation and the ligand as sticks. Acidic, polar, and hydrophobic residues comprising the binding site on MVN are colored red, sky blue, and green, respectively. The reducing and terminal mannopyranose rings are labeled A and B, respectively. *C*, bond rendering showing detailed interactions between MVN and α -mannobiose. Black dotted lines connect atoms located within hydrogen bonding distance; green dashed lines denote van der Waals surfaces. See supplemental Table S2 for structure statistics of complex. Coordinates have been deposited to the Protein Data Bank, accession no. ID 2yhh.

ted lines). When bound, both pyranose rings are in a chair conformation and stack over one another to give favorable ϕ and ψ glycosidic bond angles of 110° and -75° , respectively (48).

When the two domains are superimposed, the inability of Man α (1–2)Man to bind through domain B is apparent. Key differences detrimental to ligand binding include substitution of Gln-54 and Glu-58 in domain A with Pro-2 and His-6 in domain B. The proline residue introduces steric clash with the disaccharide and is positioned on the polar face of the mannopyranose ring, and the side chain of histidine is directed away from the binding site removing hydrogen bonding interactions with the terminal ring (supplemental Fig. S8). In addition, β -hairpin connecting strands β_9 and β_{10} in domain B is directed toward the core of the protein, whereas the equivalent in domain A curls away. Thus, residues 101–104 of domain B occlude the space that is used for carbohydrate binding in domain A.

MVN Inhibits HIV Entry through Carbohydrate-mediated Interactions with gp120—MVN was tested for its ability to inhibit HIV-1 entry in single round HIV-1 infectivity assays using a panel of CXCR4- and CCR5-using strains, and one dual tropic strain. For comparison with other known entry inhibitors, assays were run in parallel with the well characterized lectin CVN, the carbohydrate-specific monoclonal antibody 2G12 (49), and the gp41-derived peptide inhibitor C34 (50). We found MVN to potentially inhibit HIV-1 entry for all strains (Fig. 5A), with IC_{50} values of 2–12 nM (Table 3). Consistent with a recent study, MVN is slightly less potent than CVN against most strains tested and used here. In addition, MVN has comparable potency to 2G12 against all strains tested and in contrast to mAb 2G12 can inhibit strain YU2. HIV-1 strain YU2 is

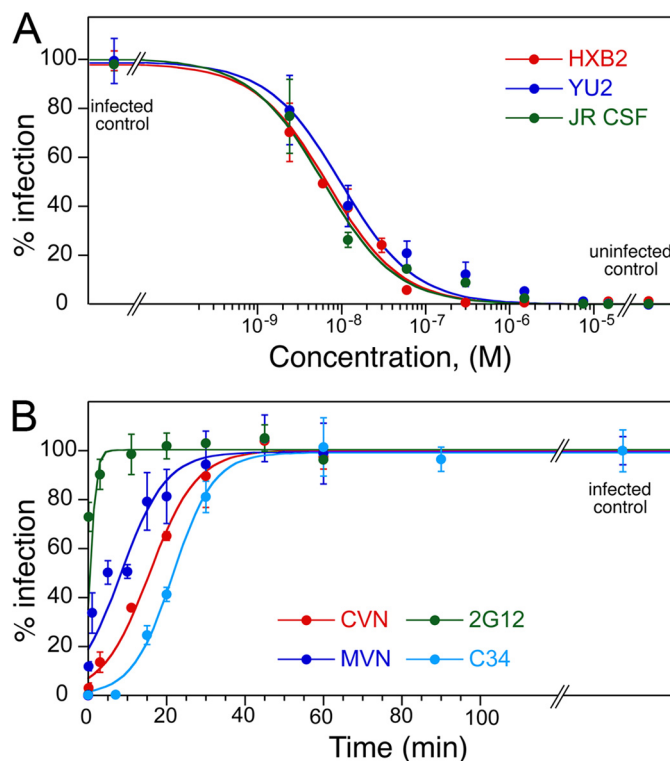


FIGURE 5. Antiviral activity of MVN in an Env-pseudotyped HIV neutralization assay. *A*, representative dose-response curves for antiviral activity of MVN against HIV pseudotyped with Env of diverse laboratory-adapted subtype B HIV strains (Table 3). *B*, infectivity as a function of time of addition of fusion inhibitors in a synchronized HXB2 Env-pseudotyped HIV infection assay. Fully inhibitory concentrations of MVN, CVN, 2G12, and C34 were added at the indicated time points. The experimental data (average of a minimum of four experiments) were fit to a sigmoidal curve (see “Experimental Procedures”). $t_{1/2}$ values of the inhibitor-sensitive state are as follows: 2G12 ≤ 1 min, MVN 8.4 ± 1.6 min, CVN 15.7 ± 1.0 min, C34 21.7 ± 0.6 min.

Solution Structure of Microvirin

TABLE 3

Inhibition of HIV-1 by MVN, CVN, 2G12, and C34

	HIV neutralization, IC ₅₀ (nM) ^a						
	Env	HXB2	NL4-3	SF162	YU2	JRCSF	
MVN	6.0 ± 0.6	1.8 ± 0.6	2.2 ± 1.0	9.9 ± 2.0	6.1 ± 1.1	11.6 ± 3.3	
CVN	0.1 ± 0.03	2.2 ± 1.5	0.5 ± 0.1	1.5 ± 0.1	1.1 ± 0.3	0.5 ± 0.2	
2G12	2.1 ± 0.3	5.5 ± 2.9	4.2 ± 2.6	No activity	6.6 ± 3.4	24.3 ± 16.7	
C34	6.3 ± 1.8	4.0 ± 0.8	60 ± 16	98 ± 25	28.2 ± 9.1	26.0 ± 6.3	

^a IC₅₀ values were obtained by least squares best fitting to the general equation: % infection = 100/(1 + [inhibitor]/K).

known to be resistant to mAb 2G12 because it lacks an Asn at position 295 of gp120, a glycosylation site involved in 2G12 binding (49).

Huskens *et al.* (22) recently showed that MVN can inhibit the binding of 2G12 to gp120 through *in vitro* binding assays. We sought to test directly whether MVN inhibits HIV-1 entry through carbohydrate-mediated interactions with gp120. Thus, competition experiments using infectivity assays were performed wherein we competed MVN with increasing amounts of Man₉GlcNAc₂ prior to combining with virus and target cells. We found that treatment with Man₉GlcNAc₂ alone had no effect on entry, but addition of excess Man₉GlcNAc₂ to MVN reduced its inhibitory effect by 20–30% (supplemental Fig. S9). Thus, Man₉GlcNAc₂ competes with gp120 for MVN binding and inhibition, demonstrating fusion-blocking activity occurs through carbohydrate-mediated interactions.

Carbohydrate-targeting Inhibitors Act at Different Stages of the HIV Entry Process—Binding of HIV gp120 to CD4 on target cells followed by gp120 binding to coreceptor(s) CXCR4 or CCR5 via a CD4-induced coreceptor-binding site leads to HIV-1 entry. Conformational changes occurring at each of these steps trigger HIV gp41 to its fusogenic state and drive membrane fusion. To compare the time window of inhibition of HIV-1 entry for MVN, CVN, 2G12, and C34, we performed synchronized viral entry assays using HIV-1 strain HXB2. Percent inhibition as a function of time of addition was measured to give a half-life of the inhibitor-sensitive state (*t*_{1/2}) for each of the four inhibitors (Fig. 5B). 2G12 was found to have an immeasurably short *t*_{1/2}, consistent with its high dependence on gp120 conformation (49). C34 had the longest *t*_{1/2}, as it targets the gp41 pre-hairpin intermediate that persists until the late stages of entry (4, 51). Although both target high mannose oligosaccharides on gp120, MVN and CVN showed distinctly different half-lives, with values of ~8 and ~16 min, respectively. These data show that MVN and CVN inhibit entry with different kinetics, suggesting that the two lectins may target different glycans on gp120, that the architecture or accessibility of each of their carbohydrate epitope(s) changes over the course of the entry process, or some combination of each.

MVN, CVN, and 2G12 Can Target Different Carbohydrates on gp120—To further probe whether MVN, CVN, and 2G12 recognize the same or distinct glycosylation sites on gp120, we tested the inhibitors individually and in constant ratio combinations for their effects on HIV-1 strain HXB2. The data were quantitatively analyzed using the formalism of Chou and Talalay (41) where combination indices (CI) equal to, greater than, or less than 1 are indicative of additive, antagonistic, and synergistic effects, respectively. Fig. 6A displays the results of testing combinations of MVN and 2G12 and Fig. 6B combinations

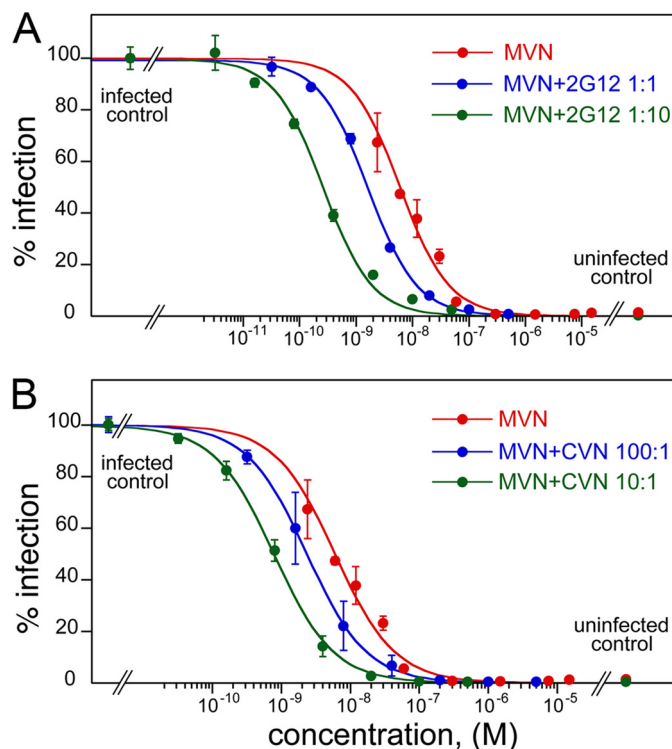


FIGURE 6. MVN is synergistic with 2G12 (A) and CVN (B). Combination ratios are shown in the figure and listed in Table 3, and combination indices are summarized in Table 4 and supplemental Table S3.

of MVN and CVN. For all combinations, mildly synergistic inhibition occurs with CIs ranging from 0.6 to 0.8 (Table 4 and supplemental Table S3). The mean CI value obtained for all assays is 0.7 ± 0.1 . If each of these inhibitors were acting by binding to the same carbohydrates, antagonistic effects would be expected to occur, in contrast with these data.

Effects of MVN and CVN on Other Enveloped Viruses—Neutralization assays using two amphotropic enveloped viruses, murine leukemia virus (MLV) and vesicular stomatitis virus (VSV), were performed as controls to test the specificity of MVN and CVN toward viral entry. Both MLV and VSV possess glycosylated envelope proteins yet contain many fewer glycosylation sites than gp120 (52, 53). Dramatically different effects were observed for the two lectins; and although MVN had no effect on entry for either virus at concentrations as high as 10 μ M, CVN inhibited entry for both in a dose-dependent manner with IC₅₀ values of 21 ± 3 nM for MLV and 190 ± 80 nM for VSV (supplemental Fig. S10). Because the carbohydrate-binding site of MVN is very similar to its equivalent in domain A of CVN, these results suggest that the difference in activity toward these enveloped viruses may be attributed to the lack of the second carbohydrate-binding site in MVN.

TABLE 4
Synergistic activity of MVN in combination with CVN, 2G12

All experiments were performed as described previously (42) using HXB2 Env-pseudotyped HIV.

Concentration ratios	DRI ^a		CI ^b
	MVN	CVN	
MVN:CVN			
1	85.7 ± 25.9	1.7 ± 0.5	0.6 ± 0.3
10	9.4 ± 2.0	2.0 ± 0.4	0.7 ± 0.2
100	2.5 ± 0.4	6.0 ± 1.1	0.6 ± 0.2
MVN:2G12			
10	1.5 ± 0.3	9.5 ± 1.9	0.8 ± 0.3
1	5.0 ± 1.3	3.2 ± 0.9	0.6 ± 0.2
0.1	28.6 ± 6.1	1.8 ± 0.4	0.6 ± 0.2

^a The DRI is the ratio of the IC₅₀ in the absence and presence of the second inhibitor. The IC₅₀ values for MVN, CVN, 2G12 alone are 6.0 ± 0.6, 0.1 ± 0.01, and 3.8 ± 0.4, respectively.

^b The CI represents the combined effect of two inhibitors in combination where CI values of <1, 1, and >1 correspond to synergistic, additive, and antagonistic effects, respectively (41).

DISCUSSION

In this study, we used NMR, biophysical techniques, and HIV-1 infectivity assays to determine the structural and mechanistic basis for the antiviral activity of MVN. This cyanobacterial lectin has been proposed as a candidate for development as a topical microbicide because of its ability to potently inhibit HIV-1 entry with negligible toxicity. Although MVN is a member of the CVN family of lectins, it possesses distinct structural characteristics compared with CVN that we propose account for its low toxicity and narrow antiviral profile.

As shown by complementary biophysical measurements, MVN exists as a monodisperse monomer in solution with no trace of dimeric protein present. MVN contains only one carbohydrate recognition site, and it is specific for Man α (1–2)Man, the disaccharide unit that terminates the arms of high mannose *N*-linked oligosaccharides. Unlike its homolog CVN, which contains two Man α (1–2)Man recognition sites on symmetrically opposed domains of the protein, MVN is unable to cross-link branched oligomannosides to form higher order structures. Indeed, we were able to monitor the binding of MVN to the branched oligomannoside Man₈GlcNAc₂ by NMR due to the absence of polymerization. Together, these data are consistent only with monovalent binding. In addition, because MVN binds the HIV surface envelope glycoprotein gp120, and its antiviral activity can be competed with Man₈GlcNAc₂, these data demonstrate that HIV-1 entry can be inhibited through monovalent interactions with carbohydrates on gp120.

Our time of addition studies show that different carbohydrate-binding agents can interact with the HIV viral envelope at different stages of the entry process. Once CD4 is engaged, 2G12, known to recognize a specific architecture of clustered glycans displayed on one face of gp120, has an immeasurably short window of time in which it can inhibit entry. Thus, conformational changes associated with CD4 binding must immediately disrupt the carbohydrate epitope of 2G12 on fusogenic gp120. MVN and CVN can inhibit virus entry up to substantially longer periods of time, but the shorter inhibitor-sensitive state observed for MVN suggests its carbohydrate epitopes are shorter lived than those of CVN.

On a molecular level, nonequivalent modes of binding and mechanisms of inhibition must be occurring to explain the dis-

parate kinetics exhibited by MVN, CVN, and 2G12. These could include binding of different glycans on gp120 by each inhibitor or targeting distinct conformations of overlapping or even identical glycans on gp120 that change during the course of entry. Our observation that each of these inhibitors can act synergistically with one another in neutralization assays shows that they must in part exert their action by binding nonoverlapping glycans on gp120 and emphasizes the difference between *in vitro* binding versus neutralization platforms. Our results are consistent with a recent study showing that distinct sets of mutations, all of which eliminated glycosylation sites on HIV-1 strain NL43, arose to confer resistance to 2G12, CVN, and MVN (22). In particular, a single mutation of Asn-295 conferred resistance to 2G12; a pair of mutations at Asn-339 and -386 led to CVN resistance, and four mutations at Asn-295, -339, -386, and -392 were observed in MVN-resistant mutants. Given that each of these inhibitors is specific for the Man α (1–2)Man termini of high mannose oligosaccharides, it is remarkable that each of these carbohydrate-binding agents appears to inhibit HIV entry through a unique set of interactions with gp120 and possibly gp41.

CVN in particular is known to inhibit many viruses besides HIV, examples of which include influenza (54), herpes (55), and hepatitis C (56). To compare the effects of valency on inhibition of enveloped viruses, we tested MVN and CVN in parallel against MLV and VSV, enveloped viruses that also display glycosylated envelope proteins. The observation that CVN inhibited both in a dose-dependent manner whereas MVN had no effect at concentrations as high as 10 μ M (supplemental Fig. S10) strongly suggests that bivalent interactions achievable with CVN but not MVN occur and are necessary for inhibition of these viruses. In contrast, the potency of MVN toward HIV-1 implies that gp120 acts as a clustered glycan epitope (19, 20, 57) to facilitate high avidity binding, even with monovalent receptors. It is conceivable that the differences in valency also account for differences in toxicity toward some cell lines as multivalent lectins can cause receptor clustering, which in turn can lead to mitogenic effects (58). These results also emphasize the selectivity that can be shown by lectins and other carbohydrate-binding agents where recognition in biological systems is imparted by geometry and spatial organization of carbohydrate recognition sites, in addition to carbohydrate specificity of the site itself. Indeed, the bacterial lectin actinohivin (unrelated to the proteins described here), which also recognizes Man α (1–2)Man, exerts its anti-HIV activity with yet a different mechanism (12) than MVN, CVN (11), and 2G12 (49).

In summary, this work describes the structural and functional basis for potent inhibition of HIV-1 entry by MVN and expands our understanding of carbohydrate-mediated inhibition by well studied anti-HIV agents CVN and 2G12. The structure of the carbohydrate recognition domain provides an attractive template for engineering smaller molecules for carbohydrate recognition. The distinct manner in which various antiviral lectins or antibodies exert their inhibitory effects on HIV continues to illustrate new mechanisms by which carbohydrate-mediated inhibition and binding can occur.

Acknowledgments—We thank D. Smith of the Consortium for Functional Glycomics for glycan microarray data and C. Schweiters and D. Garrett, National Institutes of Health, for software support.

REFERENCES

- Taiwo, B., Hicks, C., and Eron, J. (2010) *J. Antimicrob. Chemother.* **65**, 1100–1107
- Folkers, G. K., and Fauci, A. S. (2010) *JAMA* **304**, 350–351
- Balzarini, J. (2007) *Nat. Rev. Microbiol.* **5**, 583–597
- Chan, D. C., and Kim, P. S. (1998) *Cell* **93**, 681–684
- Leonard, C. K., Spellman, M. W., Riddle, L., Harris, R. J., Thomas, J. N., and Gregory, T. J. (1990) *J. Biol. Chem.* **265**, 10373–10382
- Yeh, J. C., Seals, J. R., Murphy, C. I., van Halbeek, H., and Cummings, R. D. (1993) *Biochemistry* **32**, 11087–11099
- Mizuochi, T., Matthews, T. J., Kato, M., Hamako, J., Titani, K., Solomon, J., and Feizi, T. (1990) *J. Biol. Chem.* **265**, 8519–8524
- Scanlan, C. N., Offer, J., Zitzmann, N., and Dwek, R. A. (2007) *Nature* **446**, 1038–1045
- O’Keefe, B. R., Vojdani, F., Buffa, V., Shattock, R. J., Montefiori, D. C., Bakke, J., Mirsalis, J., d’Andrea, A. L., Hume, S. D., Bratcher, B., Saucedo, C. J., McMahon, J. B., Pogue, G. P., and Palmer, K. E. (2009) *Proc. Natl. Acad. Sci. U.S.A.* **106**, 6099–6104
- Tsai, C. C., Emau, P., Jiang, Y., Agy, M. B., Shattock, R. J., Schmidt, A., Morton, W. R., Gustafson, K. R., and Boyd, M. R. (2004) *AIDS Res. Hum. Retroviruses* **20**, 11–18
- Bewley, C. A., and Otero-Quintero, S. (2001) *J. Am. Chem. Soc.* **123**, 3892–3902
- Tanaka, H., Chiba, H., Inokoshi, J., Kuno, A., Sugai, T., Takahashi, A., Ito, Y., Tsunoda, M., Suzuki, K., Takénaka, A., Sekiguchi, T., Umeyama, H., Hirabayashi, J., and Omura, S. (2009) *Proc. Natl. Acad. Sci. U.S.A.* **106**, 15633–15638
- Bewley, C. A., Cai, M., Ray, S., Ghirlando, R., Yamaguchi, M., and Muramoto, K. (2004) *J. Mol. Biol.* **339**, 901–914
- Mori, T., O’Keefe, B. R., Sowder, R. C., 2nd, Bringans, S., Gardella, R., Berg, S., Cochran, P., Turpin, J. A., Buckheit, R. W., Jr., McMahon, J. B., and Boyd, M. R. (2005) *J. Biol. Chem.* **280**, 9345–9353
- Lee, Y. C., and Lee, R. T. (1995) *Acc. Chem. Res.* **28**, 7
- Kiessling, L. L., and Pohl, N. L. (1996) *Chem. Biol.* **3**, 71–77
- Kitov, P. I., Sadowska, J. M., Mulvey, G., Armstrong, G. D., Ling, H., Pannu, N. S., Read, R. J., and Bundle, D. R. (2000) *Nature* **403**, 669–672
- Brewer, C. F., Miceli, M. C., and Baum, L. G. (2002) *Curr. Opin. Struct. Biol.* **12**, 616–623
- Dam, T. K., and Brewer, C. F. (2008) *Biochemistry* **47**, 8470–8476
- Dam, T. K., Gerken, T. A., and Brewer, C. F. (2009) *Biochemistry* **48**, 3822–3827
- Kehr, J. C., Zilliges, Y., Springer, A., Disney, M. D., Ratner, D. D., Bouchier, C., Seeberger, P. H., de Marsac, N. T., and Dittmann, E. (2006) *Mol. Microbiol.* **59**, 893–906
- Huskens, D., Féfir, G., Vermeire, K., Kehr, J. C., Balzarini, J., Dittmann, E., and Schols, D. (2010) *J. Biol. Chem.* **285**, 24845–24854
- Bewley, C. A. (2001) *Structure* **9**, 931–940
- Bewley, C. A., Kiyonaka, S., and Hamachi, I. (2002) *J. Mol. Biol.* **322**, 881–889
- Schuck, P. (2000) *Biophys. J.* **78**, 1606–1619
- Cole, J. L., Lary, J. W., P, Moody, T., and Laue, T. M. (2008) *Methods Cell Biol.* **84**, 143–179
- Delaglio, F., Grzesiek, S., Vuister, G. W., Zhu, G., Pfeifer, J., and Bax, A. (1995) *J. Biomol. NMR* **6**, 277–293
- Garrett, D. S., Powers, R., Gronenborn, A. M., and Clore, G. M. (1991) *J. Magn. Reson.* **95**, 214–220
- Schwieters, C. D., Kuszewski, J. J., and Clore, G. M. (2006) *Prog. Nucl. Magn. Reson. Spec.* **48**, 47–62
- Shen, Y., Delaglio, F., Cornilescu, G., and Bax, A. (2009) *J. Biomol. NMR* **44**, 213–223
- Ruckert, M. (2000) *J. Am. Chem. Soc.* **122**, 4
- Ottiger, M., Delaglio, F., and Bax, A. (1998) *J. Magn. Reson.* **131**, 373–378
- Kay, L. E., Torchia, D. A., and Bax, A. (1989) *Biochemistry* **28**, 8972–8979
- Clore, G. M., Driscoll, P. C., Wingfield, P. T., and Gronenborn, A. M. (1990) *Biochemistry* **29**, 7387–7401
- Schwieters, C. D., and Clore, G. M. (2001) *J. Magn. Reson.* **152**, 288–302
- Shahzad-ul-Hussan, S., Cai, M., and Bewley, C. A. (2009) *J. Am. Chem. Soc.* **131**, 16500–16508
- Gustchina, E., Louis, J. M., Lam, S. N., Bewley, C. A., and Clore, G. M. (2007) *J. Virol.* **81**, 12946–12953
- Li, M., Gao, F., Mascola, J. R., Stamatatos, L., Polonis, V. R., Koutsoukos, M., Voss, G., Goepfert, P., Gilbert, P., Greene, K. M., Bilska, M., Kothe, D. L., Salazar-Gonzalez, J. F., Wei, X., Decker, J. M., Hahn, B. H., and Montefiori, D. C. (2005) *J. Virol.* **79**, 10108–10125
- O’Doherty, U., Swiggard, W. J., and Malim, M. H. (2000) *J. Virol.* **74**, 10074–10080
- Reeves, J. D., Gallo, S. A., Ahmad, N., Miamidian, J. L., Harvey, P. E., Sharron, M., Pohlmann, S., Sfakianos, J. N., Derdeyn, C. A., Blumenthal, R., Hunter, E., and Doms, R. W. (2002) *Proc. Natl. Acad. Sci. U.S.A.* **99**, 16249–16254
- Chou, T. C., and Talalay, P. (1981) *Eur. J. Biochem.* **115**, 207–216
- Gustchina, E., Louis, J. M., Bewley, C. A., and Clore, G. M. (2006) *J. Mol. Biol.* **364**, 283–289
- Creighton, T. E. (1979) *J. Mol. Biol.* **129**, 235–264
- Bewley, C. A., Gustafson, K. R., Boyd, M. R., Covell, D. G., Bax, A., Clore, G. M., and Gronenborn, A. M. (1998) *Nat. Struct. Biol.* **5**, 571–578
- Percudani, R., Montanini, B., and Ottonello, S. (2005) *Proteins* **60**, 670–678
- Blixt, O., Head, S., Mondala, T., Scanlan, C., Hufleit, M. E., Alvarez, R., Bryan, M. C., Fazio, F., Calarese, D., Stevens, J., Razi, N., Stevens, D. J., Skehel, J. J., van Die, I., Burton, D. R., Wilson, I. A., Cummings, R., Bovin, N., Wong, C. H., and Paulson, J. C. (2004) *Proc. Natl. Acad. Sci. U.S.A.* **101**, 17033–17038
- Clore, G. M., and Garrett, D. S. (1999) *J. Am. Chem. Soc.* **121**, 9008–9012
- Bernardi, A., Colombo, A., and Sánchez-Medina, I. (2004) *Carbohydr. Res.* **339**, 967–973
- Calarese, D. A., Scanlan, C. N., Zwick, M. B., Deechongkit, S., Mimura, Y., Kunert, R., Zhu, P., Wormald, M. R., Stanfield, R. L., Roux, K. H., Kelly, J. W., Rudd, P. M., Dwek, R. A., Katinger, H., Burton, D. R., and Wilson, I. A. (2003) *Science* **300**, 2065–2071
- Chan, D. C., Chutkowski, C. T., and Kim, P. S. (1998) *Proc. Natl. Acad. Sci. U.S.A.* **95**, 15613–15617
- Gallo, S. A., Clore, G. M., Louis, J. M., Bewley, C. A., and Blumenthal, R. (2004) *Biochemistry* **43**, 8230–8233
- Polonoff, E., Machida, C. A., and Kabat, D. (1982) *J. Biol. Chem.* **257**, 4023–4028
- Robertson, J. S., Etchison, J. R., and Summers, D. F. (1982) *J. Gen. Virol.* **58**, 13–23
- O’Keefe, B. R., Smee, D. F., Turpin, J. A., Saucedo, C. J., Gustafson, K. R., Mori, T., Blakeslee, D., Buckheit, R., and Boyd, M. R. (2003) *Antimicrob. Agents Chemother.* **47**, 2518–2525
- Tiwari, V., Shukla, S. Y., and Shukla, D. (2009) *Antiviral Res.* **84**, 67–75
- Helle, F., Wychowski, C., Vu-Dac, N., Gustafson, K. R., Voisset, C., and Dubuisson, J. (2006) *J. Biol. Chem.* **281**, 25177–25183
- Lehotzky, R. E., Partch, C. L., Mukherjee, S., Cash, H. L., Goldman, W. E., Gardner, K. H., and Hooper, L. V. (2010) *Proc. Natl. Acad. Sci. U.S.A.* **107**, 7722–7727
- Sharon, N., and Lis, H. (2004) *Glycobiology* **14**, 53R–62R
- Clore, G. M., Gronenborn, A. M., and Bax, A. (1998) *J. Magn. Reson.* **133**, 216–221
- Laskowski, R. A., Macarthur, M. W., Moss, D. S., and Thornton, J. M. (1993) *J. Appl. Crystallogr.* **26**, 283–291